JPn Neuroscience

The Journal of Physiology

J Physiol 590.16 (2012) pp 3821–3839

Requirement of neuronal connexin36 in pathways mediating presynaptic inhibition of primary afferents in functionally mature mouse spinal cord

Wendy Bautista, James I. Nagy, Yue Dai and David A. McCrea

Spinal Cord Research Centre, University of Manitoba, Winnipeg, Manitoba R3E 0J9, Canada

Key points

- Reflexes evoked by sensory information from muscles and skin play an important role in controlling muscle activity during movement.
- The strength of these reflexes is regulated in part by presynaptic inhibition, a process controlling the release of chemical transmitters from sensory fibres terminating on spinal neurones.
- Our study is the first to show that electrical synapses among spinal neurones in young animals are essential for normal operation of processes that presynaptically regulate synaptic transmission between large diameter sensory fibres and spinal cord neurones.
- Transgenic mice lacking connexin36, a protein that mediates electrical communication via gap junctions between neurones, suffer a severe impairment of presynaptic inhibition and a similar impairment can be produced in normal mice with drugs that disrupt gap junction function.
- The wide distribution of connexin36 in the spinal cord suggests that neuronal gap junctions also play a role in other physiological processes.

Abstract Electrical synapses formed by gap junctions containing connexin36 (Cx36) promote synchronous activity of interneurones in many regions of mammalian brain; however, there is limited information on the role of electrical synapses in spinal neuronal networks. Here we show that Cx36 is widely distributed in the spinal cord and is involved in mechanisms that govern presynaptic inhibition of primary afferent terminals. Electrophysiological recordings were made in spinal cord preparations from 8- to 11-day-old wild-type and Cx36 knockout mice. Several features associated with presynaptic inhibition evoked by conditioning stimulation of low threshold hindlimb afferents were substantially compromised in Cx36 knockout mice. Dorsal root potentials (DRPs) evoked by low intensity stimulation of sensory afferents were reduced in amplitude by 79% and in duration by 67% in Cx36 knockouts. DRPs were similarly affected in wild-types by bath application of gap junction blockers. Consistent with presynaptic inhibition of group Ia muscle spindle afferent terminals on motoneurones described in adult cats, conditioning stimulation of an adjacent dorsal root evoked a long duration inhibition of monosynaptic reflexes recorded from the ventral root in wild-type mice, and this inhibition was antagonized by bicuculline. The same conditioning stimulation failed to inhibit monosynaptic reflexes in Cx36 knockout mice. Immunofluorescence labelling for Cx36 was found throughout the dorsal and ventral horns of the spinal cord of juvenile mice and persisted in mature animals. In deep dorsal horn laminae, where interneurones involved in presynaptic inhibition of large diameter muscle afferents are located, cells were extensively dye-coupled following intracellular neurobiotin injection. Coupled cells displayed Cx36-positive puncta along their processes. Our results indicate that gap junctions formed by Cx36 in spinal cord are required for maintenance of

DOI: 10.1113/jphysiol.2011.225987

presynaptic inhibition, including the regulation of transmission from Ia muscle spindle afferents. In addition to a role in presynaptic inhibition in juvenile animals, the persistence of Cx36 expression among spinal neuronal populations in the adult mouse suggests that the contribution of electrical synapses to integrative processes in fully mature spinal cord may be as diverse as that found in other areas of the CNS.

(Received 9 December 2011; accepted after revision 17 May 2012; first published online 21 May 2012)
Corresponding author D. A. McCrea: Department of Physiology, Faculty of Medicine, University of Manitoba, 745 Bannatyne Avenue, Winnipeg, Manitoba, R3E 0J9, Canada. Email: dave@scrc.umanitoba.ca

Abbreviations CDP, cord dorsum potential; Cx36, connexin36; DRP, dorsal root potential; L, lumbar; MSR, monosynaptic reflex; P, postnatal day; PAD, primary afferent depolarization; T, multiples of the weakest electrical current capable of exciting lowest threshold afferent fibres.

Introduction

It is well established that transmitter release from terminals of primary afferents in the spinal cord is subject to regulation by presynaptic inhibition (Rudomin & Schmidt, 1999). In the case of the monosynaptic reflex (MSR), the prevailing view is that presynaptic inhibition is mediated by GABAergic spinal interneurones that are located in laminae V–VI and that form axo-axonic synapses on the terminals of Ia muscle spindle afferents, as has been well established in cat (Maxwell *et al.* 1990; see Rudomin, 2009) and more recently in rodent (Hughes *et al.* 2005). Activation of these GABAergic neurones by excitatory spinal interneurones receiving large diameter muscle afferent input results in a depolarization of Ia afferent terminals and a presynaptic reduction in the monosynaptic excitation of motoneurones by Ia afferents. Afferent fibre terminal depolarization during presynaptic inhibition can be recorded extracellularly as the dorsal root potential (DRP) or intra-axonally from afferent fibres as primary afferent depolarization (PAD). PAD can also be inferred when current pulses delivered within the spinal cord become more effective in activating afferent fibres, i.e. by the Wall technique (see Willis, 2006). An important feature of presynaptic inhibition of muscle afferents is that the activity of the last order interneurones that mediate this inhibition via contact with intraspinal afferent terminals appears to be highly synchronized even though these interneurones are distributed over large distances in the spinal cord (Lidierth & Wall, 1996; see Rudomin, 2009). Here we sought to determine whether electrical coupling might play a role in the synchronization of spinal interneurones involved in the presynaptic inhibition of large diameter sensory afferents.

The occurrence and functional importance of electrical synaptic transmission between neurones in the mammalian brain has been documented in numerous studies (reviewed in Nagy & Dermietzel, 2000; Bennett & Zukin, 2004; Hormuzdi *et al.* 2004: Meier & Dermietzel, 2006). The ultrastructural correlate of electrical synapses is the gap junction, a structure composed of channel-forming connexin proteins that link the cytoplasmic compartments of coupled cells and allow cell-to-cell passage of ions, metabolites and tracer dyes (see Bennett, 1997). Among the connexin family of proteins that form gap junctions, Cx36 is selectively and most widely expressed in neurones, and has been localized ultrastructurally at inter-neuronal gap junctions (Rash *et al.* 2001*a*, 2007*a*,*b*; see Nagy *et al.* 2004). Electrical synapses mediate communication between diverse types of neurones and often occur between ensembles of GABAergic inhibitory interneurones (see Connors and Long, 2004). It is widely accepted that gap junctions between GABAergic neurones contribute to synchronizing neuronal membrane oscillations and promote synchronous network activity in various brain areas, including the cerebral cortex, hippocampus, reticular thalamic nucleus and cerebellum (reviewed in Connors & Long, 2004; Meier & Dermietzel, 2006). Gap junctions and electrical coupling between neurones have also been described in the mammalian spinal cord (Rash *et al.* 1996; Kiehn & Tresch, 2002; Lemieux *et al.* 2010), including between motoneurones in rat during development (Chang *et al.* 1999), between sexually dimorphic motoneurones (Coleman & Sengelaub, 2002), between Hb9 interneurones (Hinckley & Ziskind-Conhaim, 2006; Wilson *et al.* 2007), between preganglionic sympathetic neurones (Logan *et al.* 1996) and between motoneurones in the adult cat (Gogan *et al.* 1977). Overall, however, the role of electrical synapses formed by gap junctions in spinal cord is poorly understood, as is the involvement of Cx36 in the formation of these synapses.

In the present investigation, we explored the possibility that Cx36-containing gap junctions between spinal interneurones play a role in mechanisms associated with sensory-evoked presynaptic inhibition. *In vitro* experiments were performed in postnatal (P) 8- to 11-day-old wild-type and Cx36 knockout mice. In wild-type mice at these juvenile ages, motor systems are well developed and functionally mature; and unlike younger animals, the animal walks freely, supports its body weight and maintains its torso above the walking

surface (Jiang *et al.* 1999; Hinckley & Ziskind-Condhaim, 2006). Similarly, our casual observations are that the Cx36 knockouts move freely in their cages and can support their body weight during quadrupedal locomotion. However, a detailed characterization of phenotype in juvenile Cx36 knockout mice is not available. Nevertheless, the impact of Cx36 absence on adult mouse motor phenotype includes impairments in the olivary-cerebellar system (Van Der Glessen *et al.* 2008), in coherence of motoneurone firing during harmaline-induced tremor (Placantonakis *et al.* 2004) and in sensory-motor learning (Frisch *et al.* 2005; Zlomuzica *et al.* 2012). The use of juvenile animals allowed us to perform *in vitro* whole cord electrophysiological investigations of functionally mature spinal motor systems. Some results have been presented in abstract form (McCrea *et al.* 2009).

Methods

All experimental procedures were approved by University of Manitoba Central Animal Care Services and conformed to standards of the Canadian Council on Animal Care, with minimization of the number of animals used. All procedures also complied with the policies of *The Journal of Physiology* (Drummond, 2009) and UK regulations on animal experimentation.

Animals

Colonies of wild-type and Cx36 knockout mice, developed from C57/BL6–129SvEv mixed background (Deans *et al.* 2001), were established at the University of Manitoba through generous provision of wild-type and Cx36 knockout breeding pairs from Dr David Paul (Harvard). A total of 19 wild-type and 22 Cx36 knockout mice from ages P8–11 were used for *in vitro* electrophysiological studies. In addition, *in vitro* experiments were performed on seven P10–15 Wistar rats using procedures similar to those described in the mouse. Immunohistochemical studies used an additional nine wild-type and four Cx36 knockout mice at P8–11, and 10 wild-type and two Cx36 knockout adult (P50–55) mice.

Electrophysiological recordings and analysis

Animals were anaesthetized by intraperitoneal administration of ketamine/xylazine (100 mg kg^{-1} diluted in 0.9% saline), decapitated and eviscerated. The remaining tissue was placed in a dissection chamber and superfused continuously with cold oxygenated (95% O_2, 5% CO_2) artificial cerebrospinal fluid (ACSF) containing (in mM) NaCl (128), KCl (4), $CaCl_2$ (1.5), $MgSO_4$ (1), Na_2HPO_4 (0.5), $NaHCO_3$ (21) and D-glucose (30). The spinal cord was exposed by removing surrounding bone using a ventral approach, sparing as much of the cauda equina as possible. Ventral and dorsal roots were cut near the dorsal root ganglia. The spinal cord was transected at T3 and removed from the vertebral column. The isolated spinal cord was kept in cold ACSF for 30 min before transfer to a recording chamber dorsal side up, where it was superfused with oxygenated ACSF. The bath solution was heated gradually to 27°C.

Dorsal root potentials and monosynaptic reflexes were recorded with glass suction electrodes. Extracellular potentials were amplified 2000 times, band pass filtered (−3 db at 0.01 Hz and 300 Hz) and digitized at 2.5 kHz. Single shock stimuli were delivered to dorsal roots through suction electrodes using rectangular, constant current, 0.2 ms duration pulses. Stimulus intensity was expressed in multiples of the threshold current (T) for the afferent volley recorded on the cord dorsum (Fig. 1*Aa*).

Averages of the responses to 8–10 stimulus presentations were created off-line. Single shocks to the L2 dorsal root were delivered once every 10 s to evoke DRPs in the L3 dorsal root. In two experiments the DRP was recorded in L4 following L3 root stimulation. For the conditioning–test paradigm used for inhibition of the MSR, a suction electrode was placed on the L3 ventral root to record the MSR evoked by L3 dorsal root stimulation (the test stimulus, see Fig. 1*Ab*). Conditioning stimulation was delivered to the L2 dorsal root at intervals ranging from 5 to 200 ms preceding the test shock to inhibit the L3 MSR. Stimuli were delivered once every 2 s and presented in an alternating sequence of test stimulus alone followed by combined conditioning and test stimulation. Data analysis was performed using Origin Pro 7 (OriginLab Corp., Northampton, MA, USA) and traces were imported to Corel Draw for assembly of the figures.

PAD was assessed by monitoring changes in the excitability of intraspinal afferent fibre terminals in four wild-type and four Cx36 knockout mice. A monopolar, 15 μm diameter, tungsten electrode was inserted about 300 μm below the dorsal surface of the spinal cord and about half-way between the midline and the dorsal root entry zone (approximately 200–400 μm from the midline, see Fig. 8*A*). This electrode was used to deliver single 0.2 ms duration stimulus pulses for antidromic activation of afferent fibres (the test stimulus). The strength of the test stimulus (typically 5–7 μA) was adjusted to 1.5T for the antidromic volley recorded with a glass suction electrode on the dorsal root in the same spinal cord segment (L3 or L4). A second suction electrode on an adjacent caudal dorsal root was used to deliver (at 1.5T) conditioning stimulation. The condition–test interval was varied from 35 to 200 ms and conditioned and unconditioned test responses were averaged ($n = 18$) and plotted. An increase in the antidromic signal following conditioning stimulation of an adjacent dorsal root (1.5T, conditioning stimulus) was interpreted as an increase in

intraspinal terminal excitability caused by depolarization of afferent terminals, i.e. PAD.

Significant differences were assessed using Student's *t* test. The *P* criterion for significance was 0.05. Means are reported with standard error of the mean (SEM).

Drugs

All drugs were bath applied in the oxygenated recording chamber. Data collection did not begin until at least 30 min after drug application or drug washout. Final concentrations of applied agents were as follows: bicuculline 20 μM (Sigma-Aldrich), carbenoxolone 100 μM, and strychnine 10 μM. Mefloquine at a concentration of 5 μM was first dissolved in DMSO and then diluted in ACSF to yield a 0.1% concentration of DMSO. Controls experiments for mefloquine were done with bath application of 0.1% DMSO.

Neurobiotin injections

Slices from mouse spinal cord were prepared as previously described (Carlin *et al.* 2000; Dai *et al.* 2009). Briefly, 300 μm thick transverse slices from lumbar levels were cut using a vibrating blade microtome and maintained in the ACSF for 1 h. The slices were then transferred to a patch-clamp recording chamber mounted on the stage of an upright Olympus BX50 microscope fitted with differential interference contrast optics and epifluorescence. The chamber was perfused with ACSF at a rate of 2 ml min^{-1}, and oxygenated with 95% O_2, 5% CO_2. Neurones located in lamina IV–VI were visualized using infrared illumination and images were collected using a Hamamatsu camera controller C2400 (Bridgewater, NJ, USA) and Argus image processor. Patch electrodes fabricated from borosilicate glass (5–8 MΩ) were filled with intracellular recording solution containing (in mM): $KMeSO_4$ (150), NaCl (10), Hepes (10), EGTA (0.1), Mg-ATP (3), GTP (0.3), and 3% neurobiotin. Visualized neurones were patched and data acquired using a MultiClamp 700A patch-clamp amplifier (Molecular Devices, Sunnyvale, CA, USA). Whole cell patch recordings were made in current-clamp mode and six depolarizing square pulses (0–60 pA, 3 s duration) were applied for intracellular passage of neurobiotin. Negative pressure was used on the pipette before impalement and making the gigohm seal to prevent leakage extracellularly.

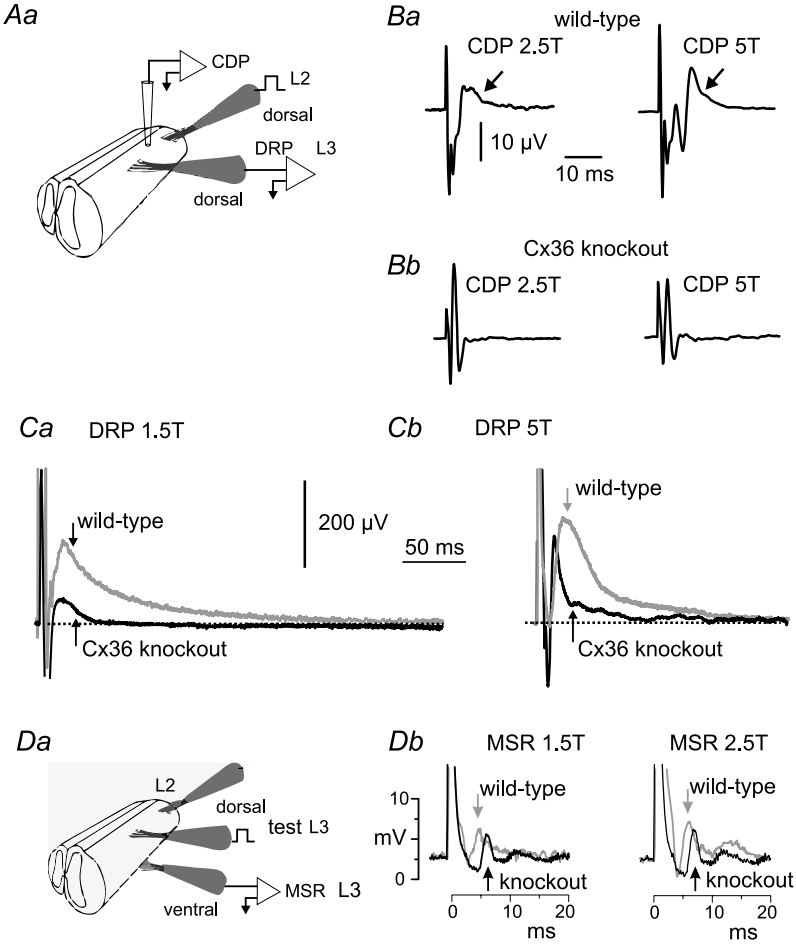

Figure 1. Experimental setup and comparison of CDP, DRP and MSR in P8–11 wild-type and Cx36 knockout mice
Aa, schematic diagram of set-up for evoking the cord dorsum potential (CDP) and dorsal root potential (DRP). *B*, CDP recorded from wild-type (*Ba*) and knockout mice (*Bb*), evoked by stimulation of the L2 dorsal root at 2.5 and 5 times the intensity of threshold for the most excitable afferents (*T*) using a rectangular current pulse 0.2 ms in duration. Arrows indicate the longer latency components seen in wild-type mice, but which are absent in Cx36 knockout mice. *C*, DRP recorded in L3 from a P10 wild-type mouse (grey trace) following single shock stimulation at 1.5*T* (*Ca*) and 5*T* (*Cb*) of the L2 dorsal root overlaid on the DRP from a Cx36 knockout mouse (*Ca* and *Cb*, black trace). The DRP is attenuated and short lasting in mice lacking Cx36. *Da*, schematic diagram of set-up for evoking monosynaptic reflexes (MSRs) in L3 and for stimulation of the L2 dorsal root for evaluating the effects of conditioning stimulation on the monosynaptic reflex. *Db*, reflexes recorded from the L3 ventral root evoked by stimulation of the L3 dorsal root. Grey traces, averaged responses from a wild-type mouse; black traces, from a Cx36 knockout mouse. Arrows indicate the point of MSR amplitude measurement. In this and following figures, stimulus artefacts are truncated for illustration purposes.

The slices were then immersion fixed for 20 min in cold 0.16 M sodium phosphate buffer, pH 7.1, containing 2% freshly depolymerized paraformaldehyde and 0.2% picric acid, and then transferred to 10 ml of 25 mM sodium phosphate buffer, pH 7.1, containing 10% sucrose. Slices were sectioned at a thickness of 15 μm using a cryostat. Sections were blocked by incubation in 10% normal goat serum for 30 min, then incubated for 1.5 h with streptavidin-conjugated AlexaFluor-488 (Jackson Immunoresearch Laboratories Inc.,West Grove, PA, USA) diluted 1:2000 in 50 mM Tris-HCl buffer, pH 7.4, containing 1.5% sodium chloride and 0.3% Triton X-100 (TBSTr) to detect neurobiotin. The sections were then processed for immunohistochemical detection of Cx36, as described below.

Immunohistochemistry

Juvenile and adult mice were deeply anaesthetized by intraperitoneal injection of ketamine/xylazine (100 mg kg^{-1} in 0.9% saline solution) and decapitated. Spinal cords were removed after exposure following laminectomy, immersion fixed for 20 min in 40 ml of cold 0.16 M sodium phosphate buffer, pH 7.1, containing 2% freshly depolymerized paraformaldehyde and 0.2% picric acid, and cryoprotected for at least 24 h in 10 ml of 25 mM sodium phosphate buffer, pH 7.4, containing 10% sucrose. Sections of lumbar regions of the spinal cord were cut at a thickness of 10 μm using a cryostat, collected on gelatinized glass slides and stored at –34°C until use. Sections were thawed, washed for 20 min in TBSTr, and then incubated for 24 h at 4°C with mouse monoclonal antibody against Cx36 (Invitrogen/Zymed Laboratories, Carlsbad, CA, USA) diluted to 2 μg ml^{-1} in TBSTr containing 5% normal donkey serum. Sections were then washed for 1 h in TBSTr and incubated for 1.5 h at room temperature with Cy3-conjugated goat anti-mouse IgG (Jackson ImmunoResearch Laboratories) diluted 1:200 in TBSTr. After secondary antibody incubations, sections were washed in TBSTr for 20 min, followed by two 15 min washes in 50 mM Tris-HCl buffer, pH 7.4, and coverslipped after application of antifade medium. For double immunofluorescence labelling, sections were incubated with rabbit polyclonal anti-peripherin (Chemicon, Temecula, CA, USA) and simultaneously with mouse monoclonal anti-Cx36 for 24 h at 4°C. Sections were then washed in TBSTr for 1 h at room temperature and incubated for 1 h simultaneously with Alexa Fluor 488-conjugated goat anti-rabbit IgG (Molecular Probes, Eugene, OR, USA) diluted 1:1000, in combination with Cy3-conjugated goat anti-mouse IgG (Jackson ImmunoResearch Laboratories) diluted 1:200. Prior to coverslipping, some sections processed for immunolabelling of Cx36 were counterstained with green Nissl fluorescent NeuroTrace (stain N21480; Molecular Probes, Eugene, OR, USA). Fluorescence was examined on a Zeiss Axioskop2 fluorescence microscope with image capture using Axiovision 3.0 software (Carl Zeiss Canada, Toronto, Ontario, Canada), or an Olympus Fluoview IX70 confocal microscope with image capture using Olympus Fluoview software (Markham, Ontario, Canada). Adobe Photoshop and Corel Draw software (Corel Corp., Ottawa, Ontario, Canada) were used for image analyses.

Results

Characteristics of DRP, CDP, MSR inhibition and PAD in wild-type mice

Much of our present knowledge of the organization, mechanism and operation of presynaptic inhibition in the spinal cord originates from observations made over many years in adult cats. The physiology and pharmacology of spinal presynaptic inhibitory systems in juvenile mouse have not been systematically analysed. Therefore, before exploring a potential role of Cx36 in these systems, we first determined whether presynaptic inhibition in the juvenile mouse displays features similar to those described in the adult cat.

The cord dorsum potential (CDP) recorded from the surface of the spinal cord was used as a reference from which to measure latencies, to determine stimulus intensity and to assess activity of dorsally located spinal neurones. Using the recording set-up described in Fig. 1*Aa*, representative CDPs shown in Fig. 1*Ba* from a wild-type mouse were produced by single-shock L2 dorsal root stimulation at 2.5 and 5 times the intensity required for activation of the lowest threshold afferents (*T*). Note the later component (arrow) that follows the large initial and brief deflection produced by the arrival of the afferent volley. The longer latency CDP component reflects population activity in dorsal horn interneurones (Manjarrez *et al.* 2003), which increases with increased stimulus intensity (Fig. 1*Ba*, left and right).

In the cat, depolarization of spinal sensory afferent terminals during presynaptic inhibition produces the DRP – a long lasting, negative going, potential recorded from a dorsal spinal root (Rudomin & Schmidt, 1999; see Rudomin, 2009). Figure 1*Aa* shows the experimental set-up used to evoke DRPs in the *in vitro* preparation. An example of a DRP evoked by single shock stimulation of the L2 dorsal root and recorded in the L3 root in a wild-type P10 mouse is shown in Fig. 1*Ca* and *b* (grey traces). The duration of the DRP evoked by 1.5*T* stimulation was 235 ± 23 ms (SEM) ($n = 19$ preparations) in juvenile wild-type mice, with a time to peak of 25 ± 3 ms. These values are similar to those reported in the adult cat (Eccles *et al.* 1963) but somewhat shorter than values reported in the spinal cord of neonatal rat (Kremer & Lev-Tov, 1998). Increasing stimulus intensity

increased DRP amplitude (Fig. 1*Cb*). Because of the known involvement of GABAergic transmission in presynaptic inhibition and the DRP in the cat (Eccles *et al.* 1963; Rudomin *et al.* 1990) and the hamster (Bagust *et al.* 1985), the effects of bath application of the GABAa antagonist, bicuculline, were examined on the DRP in the juvenile mouse *in vitro* preparation. The traces in Fig. 2*A* (left) show a modest reduction in the amplitude of the 1.5*T* evoked DRP amplitude with bath application of bicuculline. On average (Fig. 2*A*, bar graphs) the peak amplitude of the DRP evoked by 1.5*T* stimulation was decreased by 21% and that of the DRP evoked by 2.5*T* was decreased by 36% ($n = 4$) by 20 μM bicuculline. These results in juvenile mice are in agreement with the actions of $GABA_A$ antagonists on the DRP in neonatal rat and mouse whole cord preparations (Kremer & Lev-Tov, 1998; Wong *et al.* 2001) and those in the cat using picrotoxin (Eccles *et al.* 1963; Rudomin *et al.* 1990) and bicuculline (Curtis *et al.* 1971), but the degree of depression is less than that reported in the hemisected spinal cord of neonatal (P7–14) rats (Shreckengost *et al.* 2010).

Single shock stimulation of the L3 dorsal root was used to evoke a monosynaptic reflex (MSR) recorded in the L3 ventral root (Fig. 1*Da*) using rectangular pulses of 0.2 ms. The grey trace in left panel of Fig. 1*Db* shows the averaged reflex response ($n = 5$) evoked by 1.5*T* stimulation in a wild-type mouse. Increasing the stimulus intensity to 2.5*T* (Fig. 1*Db*, right panel, grey trace) resulted in growth of the early component as well as a later component. Wang *et al.* (2008) using electrical stimulation of the peripheral nerve, determined that the central latency of monosynaptic EPSP onset in motoneurones in P7 mice is about 2.8 ms (4.3 ms total latency minus 1.5 ms afferent conduction time). The central latency of a disynaptic (inhibitory) pathway (Wang *et al.* 2008) is about 6.3 ms. In Fig. 1*Db*, the latency of the earliest reflex response, as measured from the onset of the stimulus artefact, and recorded from the activity of motoneurones in the ventral root, was 3.8 ms in a wild-type mouse and, therefore, clearly a monosynaptic reflex. The mean latency of the MSR in 16 wild-type mouse experiments was 3.67 ± 0.42 ms.

In the cat, presynaptic inhibition of extensor monosynaptic reflexes can be evoked by brief stimulus trains to a flexor nerve (see McCrea *et al.* 1990; Rudomin *et al.* 1990). In the present study, the peak amplitude of the L3 MSR (arrows Fig. 1*Db*) was measured in the absence of stimulation (control amplitude) and in the presence of a single shock to the L2 dorsal root (see Fig. 1*Da*) (conditioned amplitude). Conditioning stimulation of the L2 root at various intervals produced a long lasting inhibition of the L3 monosynaptic reflex. Figure 3*A* (squares) shows the average time course and magnitude of this inhibition in wild-type mice ($n = 6$). Single shock conditioning stimulation to the L2 dorsal root reduced the L3 monosynaptic reflex for more than 200 ms with a maximal inhibition at a conditioning–test interval of 50 ms. Inhibition at these long conditioning–test intervals is considered as more compatible with a presynaptic rather than a postsynaptic inhibition (e.g. Curtis *et al.* 1971). No attempt was made to enhance the inhibition of the MSR by increasing the number of conditioning stimulation shocks. The open circles in Fig. 3*A* are replotted data from Eccles *et al.* (1963) showing MSR inhibition evoked by a brief conditioning stimulus train to a flexor muscle nerve in the cat. Note the qualitative similarities in the time course and degree of MSR inhibition in the cat and juvenile wild-type mouse despite the differences in the species, age and stimulation parameters of the preparations.

Presynaptic inhibition of monosynaptic reflexes in the cat is antagonized by the $GABA_A$ blockers bicuculline (Curtis *et al.* 1971) and picrotoxin (Rudomin *et al.* 1990). Figure 3*B* shows the effects of bicuculline on long latency MSR inhibition in the wild-type juvenile mouse. Instead of inhibition, conditioning stimulation resulted in an

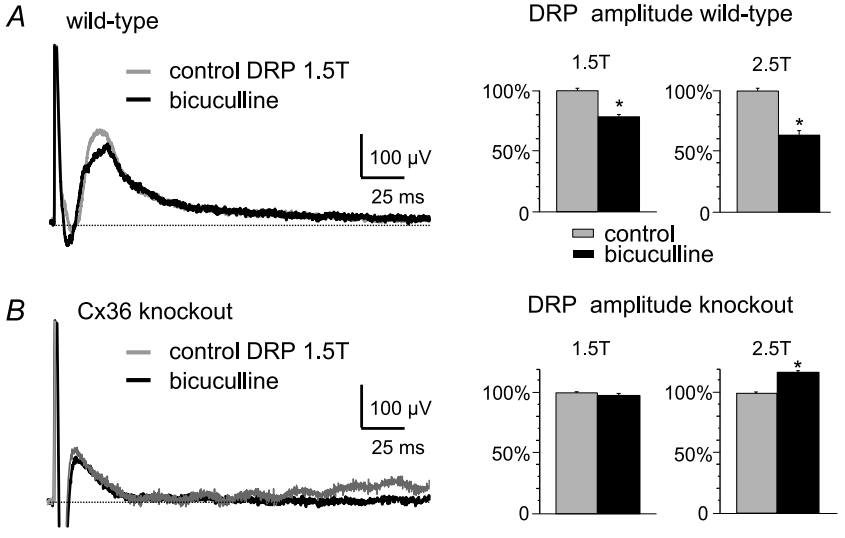

Figure 2. Effects of the $GABA_A$ antagonist bicuculline on DRPs
A and *B*, left, typical effects of bath application of 20 μM bicuculline on DRPs recorded in the fourth lumbar segment and evoked by 1.5*T* stimulation of the L3 dorsal root in wild-type mice (*A*) and Cx36 knockout mice (*B*). Right, bar graphs showing averaged effects of bicuculline on DRP amplitude from four experiments, with L3 dorsal root stimulation at 1.5*T* and 2.5*T* in wild-type mice (*A*) and Cx36 knockout mice (*B*). Results are expressed as means ± SEM; $^*P < 0.05$. The peak amplitudes of DRPs evoked by 1.5*T* and 2.5*T* stimulation were attenuated by bicuculline in wild-types (*A*, bar graphs), whereas the DRPs evoked by 1.5*T* stimulation were unaffected and those evoked by 2.5*T* stimulation were increased in knockouts (*B*).

enhancement of the MSR at longer conditioning–test intervals after bath application of 20 μM bicuculline. Bicuculline had no effect on the amplitude of the unconditioned MSR ($P = 0.81$, $n = 4$; not shown) and no effect on MSR latency (latency of 3.6 ms without bicuculline and 3.7 ms in the presence of bicuculline; $n = 4$). It is well known that conditioning stimulation can activate short-latency, postsynaptic glycinergically mediated inhibition of motoneurones. Bath application of the glycinergic blocker strychnine (10 μM) reduced MSR inhibition at short (5–20 ms) conditioning–test intervals (Curtis *et al.* 1971) but had little effect at longer intervals (not shown). The similarities of the actions of GABA antagonists and the time course of MSR inhibition in the mouse and cat suggest that the long duration inhibition evoked by low intensity dorsal root stimulation shown in Fig. 3*A* is presynaptic in origin. The shorter-latency effects of conditioning stimulation are presumably a mixture of presynaptic inhibition as well as postsynaptic inhibition and excitation (see Bagust *et al.* 1981).

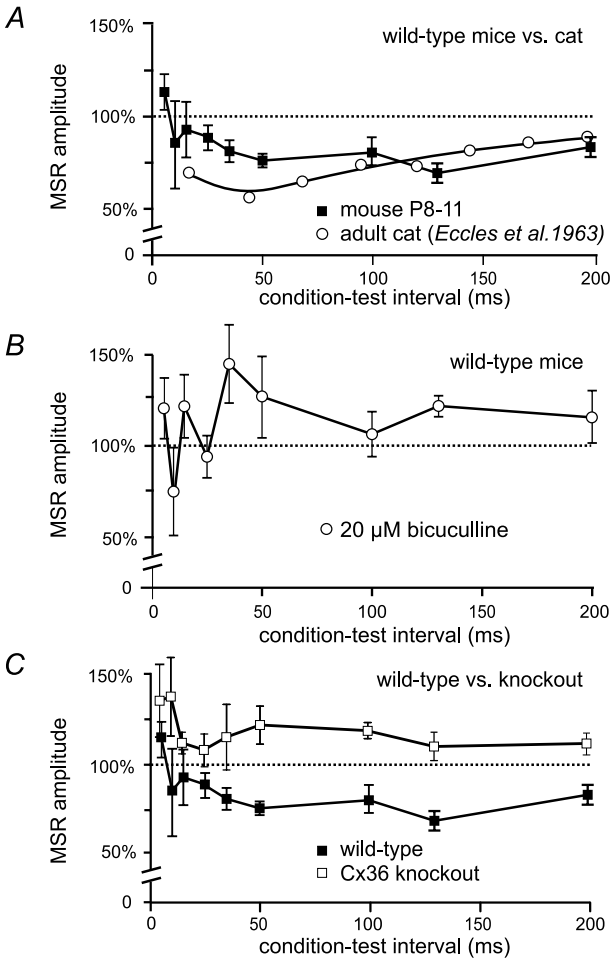

Figure 3. Effects of conditioning stimulation of the MSR in juvenile wild-type and Cx36 knockout mice
Using the paradigm outlined in Fig. 1*Da*, effects of a conditioning stimulus to the L2 dorsal root were examined on the MSR evoked by L3 dorsal root stimulation and recorded in the L3 ventral root. Normalized MSR amplitude is on the ordinate and intervals between the conditioning and test stimuli is on the abscissa. MSR amplitude is normalized to the amplitude of the unconditioned reflex. *A*, mean MSR amplitude (±SEM) following conditioning stimulation from 6 wild-type mice (filled squares). Conditioning stimulation of the L2 dorsal root in wild-types inhibits the L3-evoked MSR for more than 200 ms. Results obtained in adult cat (Eccles *et al.* 1963) are shown for comparison (open circles). *B*, bath administration of bicuculline in wild-type mice ($n = 4$) abolishes long-lasting inhibition of the MSR, showing GABAergic mediation of this inhibition. In the presence of bicuculline, values at conditioning–test intervals greater than 50 ms were significantly different from controls ($P < 0.05$). *C*, conditioning stimulation of the L2 dorsal root failed to inhibit the L3-evoked MSR in Cx36 knockout mice ($n = 7$). Results in wild-types from *A* plotted for comparison.

The increases in terminal excitability in juvenile wild-type mice are similar to the increases in excitability observed in the cat and previously in the rodent (Bagust *et al.* 1981).

In the cat (see Rudomin & Schmidt, 1999) and in the rodent (Bagust *et al.* 1981), sensory-evoked presynaptic inhibition causes a primary afferent depolarization that increases the excitability of intraspinal afferent fibre terminals. We examined changes in the excitability of primary afferent terminals in juvenile mice by comparing unconditioned intraspinally evoked antidromic afferent discharges to those conditioned by low intensity (1.5T) stimulation of an adjacent dorsal root. The upper panel in Fig. 4*A* shows the response (black arrow), recorded in the L3 dorsal root, that was evoked by a 6 μA current pulse delivered through an electrode positioned about 300 μm below the surface of the cord in a wild-type mouse. A conditioning stimulus to the L2 dorsal root delivered 35 ms before the intraspinal stimulus (Fig. 4*A*, lower trace, open arrow) resulted in an increase in the intraspinally evoked discharge (compare upper and lower traces in Fig. 4*A*). On average, conditioning stimulation almost doubled the size of the intraspinally evoked antidromic discharge (Fig. 4*C*).

DRPs, MSR inhibition and PAD in Cx36 knockout mice

The results presented in Figs 1–4 show that several characteristics of sensory-evoked presynaptic inhibition recorded in juvenile wild-type mice are similar to those involved in the same process in the adult cat. To examine the potential role of neuronal gap junctions in presynaptic inhibition, we compared results obtained in wild-type mice with those in Cx36 knockout mice.

Figure 1*B* shows representative CDPs in wild-type (*Ba*) and Cx36 knockout mice (*Bb*). Unlike the CDP in wild-type mice, the CDP in knockouts lacked the prolonged later phase and consisted primarily of just the sharp, triphasic, afferent volley. DRPs evoked by L2 dorsal root stimulation at low (Fig. 1*Ca*) and higher (Fig. 1*Cb*) stimulus intensities and recorded in the L3 dorsal root

were also severely attenuated in Cx36 null mice (compare the black and grey traces in Fig. 1*Ca* and *b*). On average, the peak amplitude of DRPs evoked by 1.5*T* stimulation in Cx36 knockout mice was smaller by 79% ($P < 0.01$; $n = 14$ wild-types and 13 knockouts). Because accurately determining the point at which a DRP returns to baseline is often difficult, comparisons between wild-type and knockout mice were made using the duration of the DRP measured at one-half of its peak amplitude. The half-amplitude duration of the DRP evoked by 1.5*T* stimulation was 24.0 ± 6.7 ms in wild-type mice ($n = 13$) and fell by 67% ($P < 0.01$) to $8.0 \text{ ms} \pm 0.6$ ms in knockout mice ($n = 14$). The duration of the 5*T* DRP was similarly affected in knockout mice, shortening by 75% (half-amplitude duration 36.6 ± 6.2 ms in wild-type mice; 8.75 ± 1.1 ms in knockout mice, $P < 0.01$). The absence of the later components of the DRP and CDP in knockout mice is consistent with reduced afferent-evoked spinal dorsal horn interneurone activity. In addition to the impairment of the DRP in knockout mice, bicuculline failed to attenuate the DRP evoked with 1.5*T* stimulation (Fig. 2*A*) while the 2.5*T* DRP became larger in the presence of the $GABA_A$ blocker in knockout mice (Fig. 2*B*, $n = 10$ in all bar graphs). We currently have no explanation for the bicuculline-induced increase in the amplitude of the higher threshold DRP.

Monosynaptic reflexes evoked by 2.5*T* dorsal root stimulation were of similar amplitude in wild-type mice and knockout mice (wild-type: 37.8 ± 4.9 μV, $n = 14$; knockout: 36.8 ± 6.9 μV, $n = 11$). The latency of the MSR was, however, longer in knock-out mice. In the example shown in Fig. 1*Db* (left panel, black trace), the latency of the reflex evoked at 1.5*T* was 4.5 ms; the average latency in 16 experiments was 4.11 ± 0.36 ms (average 3.67 ms in wild-types, see above). Because MSR latency in both wild-type and knockout mice is considerably less than the estimated latency of transmission through spinal disynaptic pathways (6.3 ms; Wang *et al.* 2008; see above), we are confident that the earliest component of the ventral root reflexes reported is monosynaptic. The longer latency responses evoked with increasing stimulus intensity in both wild-type and knock mice (compare left and right panels in Fig. 1*Db*) are likely to reflect transmission through oligosynaptic pathways. No attempt was made to measure or compare longer latency reflexes in wild-type or knockout mice in the present study. While the exact compliment of fibre types activated by electrical dorsal root stimulation in juvenile mice is unknown, it is reasonable to assume that the low intensity stimulation employed here (e.g. 1.5*T*) recruited lower threshold afferents. Supporting this view is the similarity of the MSR latencies in both wild-type and knockout mice and the latency of monosynaptic EPSPs evoked by mechanical activation of muscle afferents by Wang *et al.* (2008). It thus appears that Ia muscle spindle afferents producing monosynaptic EPSPs and monosynaptic reflexes are among the fibre types activated by low threshold dorsal root stimulation in juvenile wild-type and knockout mice.

The long lasting inhibition of the MSR produced by conditioning stimulation of an adjacent dorsal root in juvenile wild-type mice was absent in Cx36 knockout mice (Fig. 3*C*). Instead, conditioning stimulation increased the amplitude of the MSR in Cx36 knockout mice ($n = 7$) at all conditioning–test intervals examined. Bicuculline had no effect on conditioning of the MSR in Cx36 knockout mice (not shown). There is currently no information available concerning the pathways activated by the conditioning stimulus that contribute to enhancement of the MSR seen at the longer conditioning–test intervals in Cx36 knockout mice (Fig. 3*C*) or following bicuculline administration in wild-types (Fig. 3*B*).

The deficits in Cx36 knockout mice in MSR inhibition, the DRP and the CDP suggest a failure of sensory stimulation to evoke a presynaptic inhibition of sensory

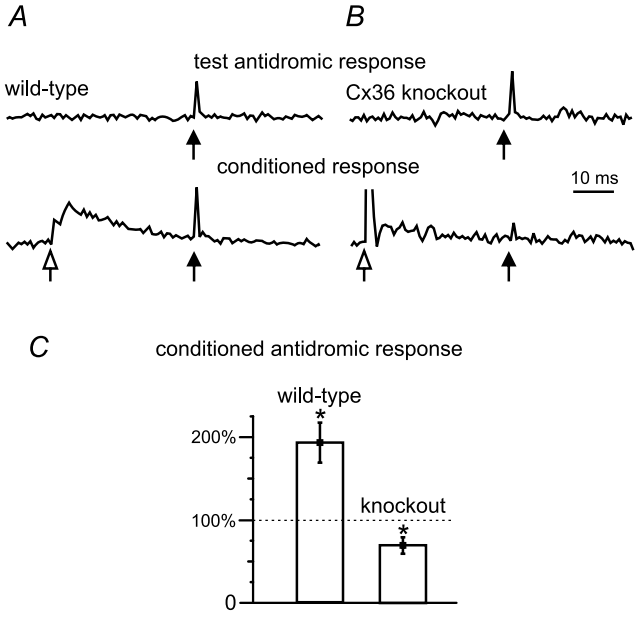

Figure 4. Primary afferent depolarization (PAD) in lumbar spinal cord of P10 wild-type and Cx36 knockout mice
A, antidromic activation of afferent fibres recorded in the L3 dorsal root following intraspinal stimulation (test, black arrow) in the dorsal horn of a wild-type mouse (upper trace). A preceding conditioning stimulus (open arrow) to the L2 dorsal root at 1.5*T* (lower trace) increased the amplitude of the intraspinally evoked antidromic signal, i.e. PAD. *B*, similar recording from a Cx36 knockout mouse shows the unconditioned antidromic activation of fibres in the dorsal root (upper trace). Conditioning stimulation decreased and often inhibited the antidromic response in knockout mice (lower trace). *C*, comparison of the effects of conditioning stimulation in wild-type *versus* Cx36 knockout mice ($P < 0.05$; $n = 6$). Values of the antidromic response >100% reflect PAD-evoked increased excitability of the afferents produced by the conditioning stimulation. Stars indicate means significantly different ($P < 0.05$) from 100% control.

afferents and hence PAD. Figure 4 compares the ability of conditioning stimulation of a dorsal root to evoke PAD in knockout and wild-type mice. Unlike the PAD produced in wild-types by conditioning stimulation of low threshold sensory afferents (Fig. 4*A*), PAD could not be evoked in Cx36 knockout mice (Fig. 4*B*). On average, the antidromic volley was decreased by conditioning stimulation in knockouts (Fig. 4*C*). Taken together, the results in Figs 1–4 suggest that Cx36, and by implication functional gap junctions, is required to produce presynaptic inhibition of large diameter afferent fibres in the lumbar spinal cord.

Action of gap junction blockers on presynaptic inhibition in wild-types

Given the above results, pharmacological blockade of gap junctions in wild-type mice would be expected to reduce presynaptic inhibition in ways similar to those observed in Cx36 knockouts. Bath application of gap junction blockers antagonized the long-latency MSR inhibition produced by conditioning stimulation and attenuated the long lasting DRP in wild-type rodents. Filled symbols in Fig. 5*A* show long latency inhibition of the MSR evoked by conditioning stimulation in wild-type mice. In the presence of 100 μM carbenoxolone (open symbols), this inhibition was antagonized at all but the shortest conditioning–test intervals. Figure 5*Ba* and *Bb* show the substantial reduction of the DRP produced by carbenoxolone in a P15 rat *in vitro* preparation. Carbenoxolone produced a similar reduction in DRP amplitude in P8–P11 wild-type mice (not shown). Mefloquine, a more selective gap junction blocker (Cruikshank *et al.* 2004), also antagonized long-latency MSR inhibition (not shown) and reversibly attenuated the DRP evoked by 1.5*T* (and 2*T*, not shown) intensity stimulation in the mouse (Fig. 5*Ca* and *b*). The positive-going DRPs in Fig. 5*Ba* and *Ca*, i.e. those going below baseline, presumably reflect a primary afferent hyperpolarization (Mendell, 1972) in the presence of gap-junction blockers. Notwithstanding concerns as to the selectivity of agents used to block gap junction channels (Juszczak & Swiergiel, 2009), the effects of gap junction blockers reported here on processes reflective of the occurrence of presynaptic inhibition parallel results observed in Cx36 knockout mice.

Immunofluorescence localization of Cx36 in spinal cord

The above results indicate that Cx36, presumably at electrical synapses formed by gap junctions between spinal neurones, plays an important role in mediating sensory-evoked presynaptic inhibition of synaptic transmission from large diameter afferents in the spinal cord of juvenile mice. Because Cx36 has not been widely described in spinal cord, we next examined the overall distribution of Cx36 in lumbar 3–5 spinal cord segments in P8–11 and adult mice using immunofluorescence labelling to detect Cx36 protein. Some sections were counterstained for Nissl fluorescence (green) with results shown either as

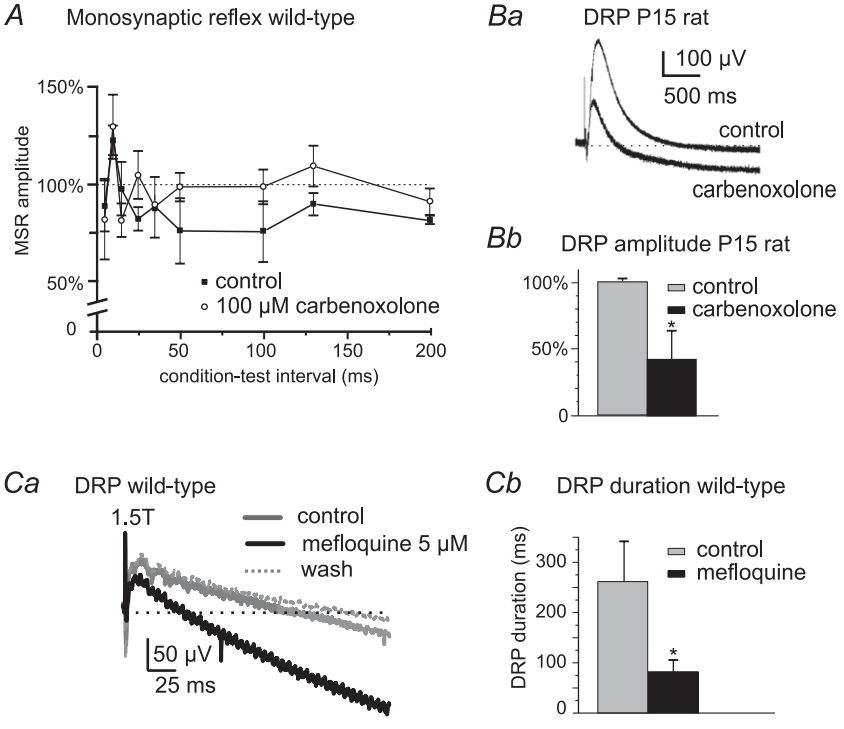

Figure 5. Gap junction blockers reduce presynaptic inhibition of the MSR and DRP amplitude in wild-type mice
A, plot showing prolonged inhibition of the L3 MSR produced by L2 stimulation at conditioning–test intervals >50 ms in P9 wild-type mice (filled symbols) and abolition of this long-lasting MSR inhibition by carbenoxolone (open symbols, $n = 3$). *Ba*, example of the depressive actions of carbenoxolone on a DRP recorded in L4 and evoked by 2*T* stimulation of the third lumbar dorsal root in a P15 rat. *Bb*, summary of effects of carbenoxolone on DRP amplitude in P15 rats ($n = 7$). *Ca*, depressant action of the gap junction blocker mefloquine (5 μM) on a DRP evoked at 1.5*T* in a P9 wild-type mouse (grey trace, control; black trace, mefloquine). DRP amplitude returned to control levels after washout of mefloquine (dotted trace). *Cb*, summary of depressant actions of mefloquine on the DRP duration evoked at 1.5*T* in P9 wild-type mice ($n = 6$). *$P < 0.05$.

Nissl/Cx36 overlays, with Cx36 labelled red, or as separate corresponding images. Because results were similar in lumbar 3–5, only data from the fourth lumbar segment are illustrated.

Immunolabelling for Cx36 consisted exclusively of Cx36-immunopositive puncta, which presumably correspond to the localization of Cx36-containing gap junctions, as observed elsewhere in the CNS (Rash *et al.* 2007*a*,*b*; Kamasawa *et al.* 2006). No specific diffuse labelling for Cx36 was observed intracellularly, precluding attempts to identify Cx36-positive neurons based on their morphology, except in the case of punctate labelling associated with the surface of large motoneurones. Punctate labelling for Cx36 in P11 mice was found in most dorsal and ventral horn laminae (Fig. 6*A*). In lamina I and II (substantia gelatinosa) and the dorsal half of lamina III (Fig. 6*B* and *C*), Cx36-puncta were sparse, more faint and of finer grain compared with those in deeper layers. Intensely fluorescent Cx36-puncta were most evident in laminae IV–VI (Fig. 6*D* and *E*). Qualitatively similar results were obtained in P9 mice, although Cx36-puncta at this age were more densely distributed in most lamina (not shown). In Cx36 knockout mice examined at P9, there was a total absence of immunolabelling for Cx36 (Fig. 6*F*) in a field corresponding to that shown in Fig. 6*E*, indicating specificity of Cx36 detection at punctate sites of labelling. The weak fixation required for visualization of Cx36 immunofluorescence led to some non-specific fluorescence, particularly in cellular nuclei, which was readily distinguishable from specific labelling through comparisons of results from wild-type and Cx36 knockout mice.

Figure 7 shows punctate labelling for Cx36 in the ventral horn of P5 (Fig. 7*A*), P10 (*B*), P11 (*C* and *E*) and adult (>50 days, *D*) wild-type mice. At P5, Cx36-puncta were located between the somata of adjacent motoneurones as seen in those simultaneously immunolabelled for the protein peripherin (Fig. 7*A*), which is highly expressed in these neurones (Duflocq *et al.* 2008; Clarke *et al.* 2010). By P10, Cx36 was additionally seen in proximal dendritic areas (Fig. 7*B*). In mice at P11, lamina IX had the most heterogeneous distribution of labelling, with some areas containing only sparse Cx36-puncta, while others displayed a consistently high density of Cx36-puncta among tightly clustered neurones (Fig. 7*C*). This pattern of immunolabelling for Cx36 in lamina IX persisted in adult mice, where Cx36-puncta remained heterogeneously distributed among motor nuclei, with subsets of motoneurones exhibiting dense accumulations of Cx36-puncta, such as those shown in Fig. 7*D*. A systematic analysis of developmental changes in Cx36 labelling in various regions of the spinal cord was not made in the present study.

Other lumbar spinal cord laminae also displayed labelling for Cx36 in the adult. As seen in Fig. 8*A*, most regions contained a lower density of Cx36-puncta than seen at P11, except ventrolateral areas of the ventral horn (Fig. 8*A*) and medial areas of laminae IV to VI (Fig. 8*B*), where robust punctate labelling persisted. In medial regions of laminae IV to VI and extending into VII, particularly striking were one or two small neurones per section that had numerous Cx36-puncta on their somata and initial dendrites (Fig. 8*C*–*E*). The quality of Nissl fluorescence staining was not sufficient to determine whether these neurones exhibited inter-dendritic appositions where gap junctional coupling could potentially occur.

Association of Cx36-puncta with neurobiotin-coupled neurones

As outlined in the Introduction, the prevailing opinion is that lumbar interneurones located in intermediate laminae are responsible for sensory-evoked presynaptic inhibition of large diameter muscle afferents. The present evidence for the involvement of Cx36 in presynaptic inhibition in mouse spinal cord, together with immunofluorescence labelling for Cx36 in intermediate laminae, raises the possibility that neurones in these laminae are linked by gap junctions. To investigate this possibility, we examined tracer–dye coupling between neurones located in laminae IV to VI in slices of lumbar spinal cord at P11. Neurones were impaled and injected with neurobiotin and the tissue processed with strepavidin-Alexa488. As shown in Fig. 9*A*, injection of a single cell produced intense tracer flourescence in the injected cell and several nearby neurones. The same section immunolabelled for Cx36 (Fig. 9*B*) showed a dense distribution of Cx36-puncta among neurones in this region. Another example of neurobiotin coupling after injection of a neurone is shown in Fig. 9*C*. Higher magnification shows a cluster of coupled neurones in close apposition (Fig. 9*D*). Laser scanning confocal analysis revealed the association of Cx36-puncta with dendrites and/or soma of both neurobiotin-injected (Fig. 9*E*) and neurobiotin-coupled (Fig. 9*F*) neurones. The weak fixation conditions required for detection of Cx36 made further handling and sectioning of the thick slices with injected cells difficult. Consequently, we recovered only four of eight injected cells in cryostat sections; two of these were coupled to other cells, two were not. We succeeded in detecting Cx36-puncta on the two coupled cells.

Discussion

This study is the first to examine the role of Cx36-containing gap junctions in sensory-evoked presynaptic inhibition in the spinal cord. We demonstrate that presynaptic inhibition of large diameter primary

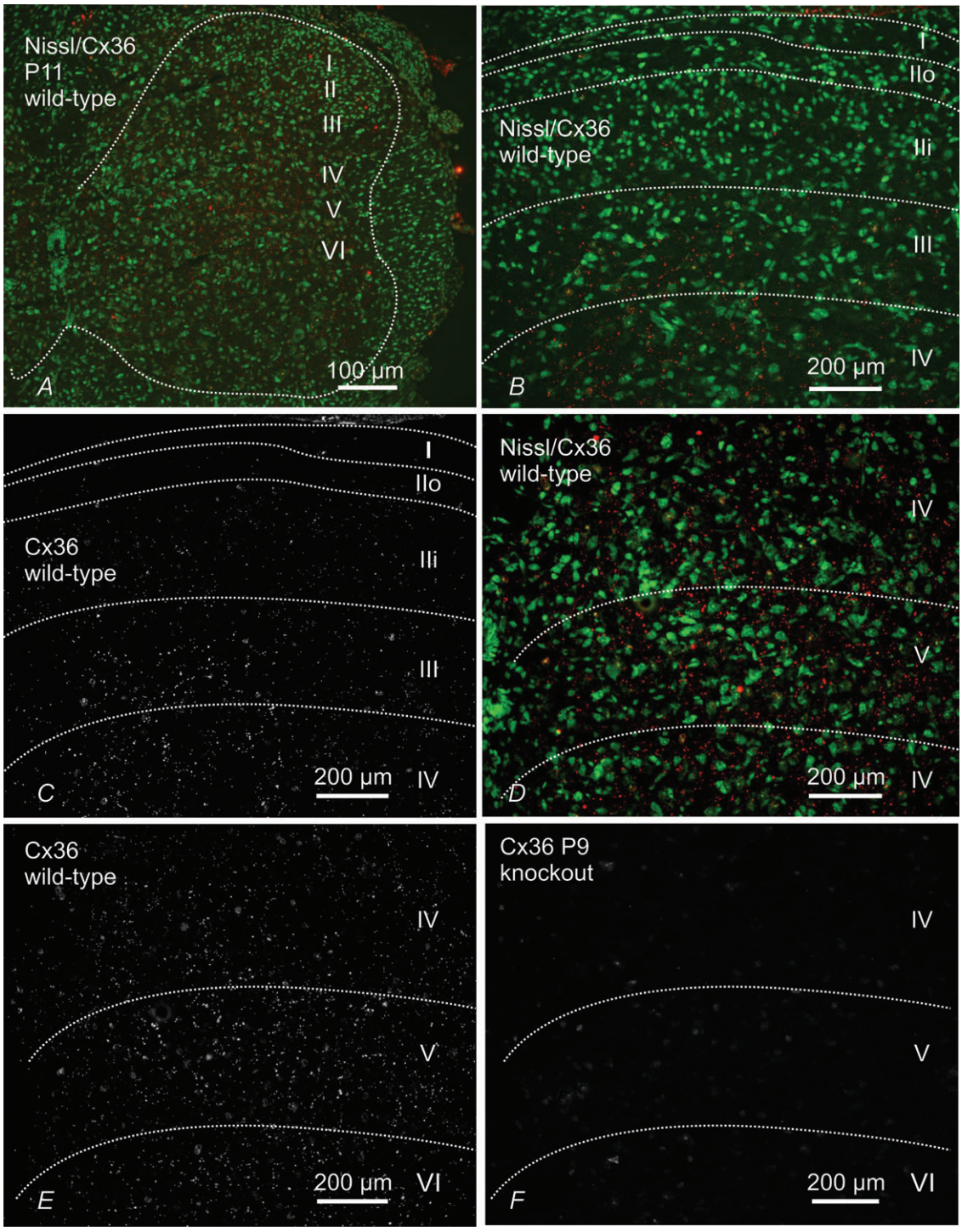

Figure 6. Immunofluorescence labelling for Cx36 in transverse sections of mouse L4 spinal cord in juvenile mice
Panels *A*–*E* are from P11 mice and panel *F* is from a P9 mouse at the fourth lumbar segment. *A*, low magnification, fluorescence Nissl counterstained section (green) showing distribution of Cx36-positive puncta (red) in dorsal and ventral grey matter (outlined by dotted line). *B* and *C*, magnification of superficial dorsal horn laminae (outlined by dotted lines) with (*B*) and without (*C*) Nissl counterstain, showing sparse labelling for Cx36 (red) in lamina I and in outer (IIo) and inner (IIi) lamina II, and moderate labelling in lamina III. *D* and *E*, magnification of deeper dorsal horn laminae (outlined by dotted lines) with (*D*) and without (*E*) Nissl counterstain, showing abundant Cx36-puncta in laminae IV, V and a portion of VI. *F*, section from the dorsal horn of a P9 Cx36 knockout mouse showing absence of labelling for Cx36 in a field similar to that shown in *E*.

afferents is dependent upon the integrity of Cx36-containg neuronal gap junctions between spinal interneurones. Longer duration components of the DRP and CDP, as well as inhibition of the MSR, were absent or substantially attenuated in Cx36 knockout mice. Because spinal motor systems in mice of the ages employed here are considered to be functionally mature (Jiang *et al.* 1999; Hinckley & Ziskind-Conhaim, 2006) and because the Cx36 immunolabelling reported here persists into adulthood, it is likely that electrical contacts between spinal interneurones also contribute to the efficacy of presynaptic inhibition in the adult.

Electrophysiology of presynaptic inhibition in wild-type and Cx36 knockout mice

Several features associated with presynaptic inhibition in wild-type *in vitro* preparations of juvenile mice are similar to those in adult cat. These include the time course of the DRP, the long-lasting inhibition of the MSR, the occurrence of sensory-evoked PAD and the attenuation of the DRP and MSR inhibition by GABA antagonists. Although the DRP is strongly associated with GABAergic mediation of presynaptic inhibition (reviewed by Rudomin & Schmidt, 1999; Rudomin, 2009), its attenuation by GABA antagonists ranges from partial (Rudomin *et al.* 1990; Thompson & Wall, 1996; Kremer & Lev-Tov, 1998; Wong *et al.* 2001; present results – Fig. 2*A*) to complete (Schreckengost *et al.* 2010). GABA antagonists can, however, very effectively attenuate the long-latency inhibition of the MSR evoked by conditioning stimulation (Fig. 3*B*; Eccles *et al.* 1963; Curtis *et al.* 1971). It remains an open question whether non-GABAergic mechanisms also contribute to presynaptic inhibition. Based on the similarities of the present results to those in the cat, it is reasonable to assume that MSR inhibition at the longer conditioning–test intervals in the mouse occurs predominately by a presynaptic mechanism. The inhibition at shorter condition test intervals (<25 ms) is likely to include a postsynaptic inhibitory component involving spinal reflex pathways (Bagust *et al.* 1981; Deshpande & Warnick, 1988; Wang *et al.* 2008).

Later components of the CDP are considered to reflect activity in dorsal horn interneurones and are correlated with activity in presynaptic inhibitory pathways (Rudomin *et al.* 1987; Enriquez *et al.* 1996). Although the shortest latency components of the CDP were qualitatively similar in wild-type and knockout mice, the later components were missing in knockouts. The absence of these components suggests a decrease in dorsal horn interneurone activity in these knockouts and in turn a reduction in the activity of presynaptic inhibitory pathways. Consistent with this suggestion, DRP duration and amplitude were decreased substantially in mice lacking Cx36 compared to wild-types of the same age. Whereas bicuculline attenuated the long lasting DRP in wild-types, the remaining short-duration DRP observed in Cx36 knockout mice was not affected by GABAa antagonists.

Presynaptic inhibition of transmitter release from large diameter primary afferent fibres in the mammalian spinal cord is mediated by GABA release at axo-axonic synapses (Rudomin, 2009), which causes a depolarization of intraspinal afferent fibre terminals, i.e. produces PAD. Consistent with the shortened and attenuated DRP in juvenile Cx36 knockout mice, PAD could not be evoked in lumbar primary afferent terminals of these mice. In wild-types, the ability of the gap junction blockers to

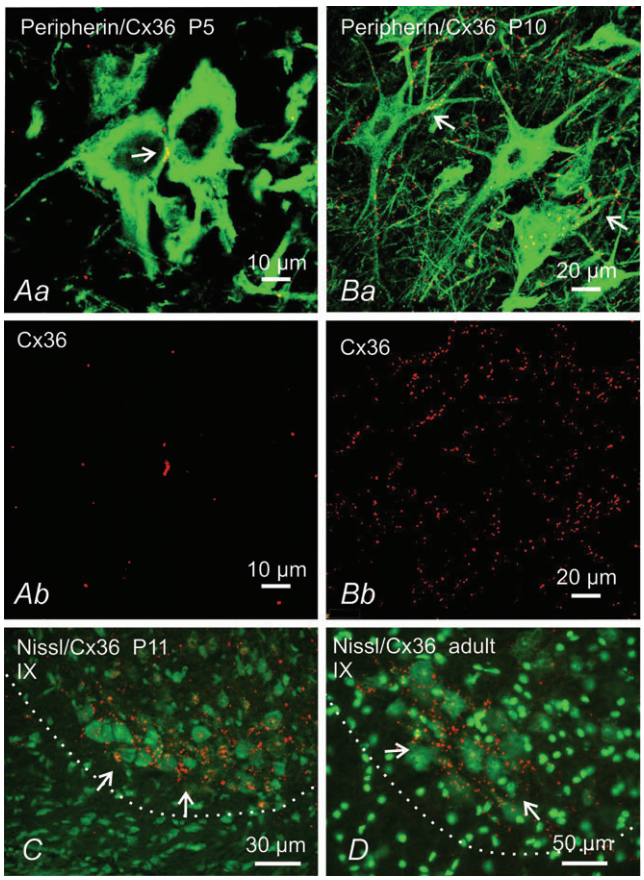

Figure 7. Immunofluorescence labelling of Cx36 in mouse spinal cord ventral horn at different developmental stages
Aa and *Ba*, laser scanning confocal overlay images showing double immunofluorescence labelling for Cx36 (red) and the motoneurone marker peripherin (green) at P5 (*Aa*) and P10 (*Ba*). *Ab* and *Bb* show only the Cx36 labelling (red) from images in *Aa* and *Ba*, respectively. At P5 motoneurones display Cx36-puncta at points of somal contact. At P10, Cx36-puncta are on somata and initial dendrites of motoneurones (*Ba*, arrows). *C*, Nissl counterstained (green) sections showing dense labelling for Cx36 (red) in lamina IX at P11 among a cluster of neurones in the ventrolateral region of lamina IX (arrows), and persistence of these puncta in adult (*D*, arrows). Border between ventrolateral grey and white matter is shown by dotted line.

antagonize the MSR inhibition evoked by conditioning stimulation (Fig. 5*A*) and reduce the DRP (Fig. 5*B* and *C*) provides further support for a critical involvement of neuronal gap junctions in presynaptic inhibition of large diameter sensory afferents.

Cx36 in juvenile and adult mice

There are a number of reports on electrical coupling between neurones in the spinal cord, but there is little anatomical information available on the expression of Cx36 in the cord. Motoneurones in rat express Cx36 mRNA (Chang *et al.* 1999), and diffuse, intracellular labelling for Cx36 protein has been detected in these neurones (Marina *et al.* 2008). Here we demonstrate a much broader distribution of Cx36 in the spinal cord of both developing and adult mouse. Importantly, as elsewhere in the CNS (Li *et al.* 2004; Rash *et al.* 2004, 2007*a*,*b*), we found that specific immunofluorescence labelling for Cx36 in spinal cord (i.e. that which was absent in Cx36 knockout mice) consisted exclusively of Cx36-puncta. Presumably these puncta reflect localization of Cx36 to neuronal gap junctions that have been shown ultrastructurally to contain Cx36 (Rash *et al.* 2001*a*,*b*; Nagy *et al.* 2004).

Although spinal neurones may express other connexins (see Chang *et al.* 1999), the DRP and lasting inhibition of the MSR were severely affected by the absence of Cx36. It thus appears that Cx36 is critically involved in the physiological processes examined here. In other CNS regions and in the spinal cord, developmental decreases in electrical coupling and down-regulation of Cx36 expression are well described (Walton & Navarrete, 1991; Kandler & Katz, 1995; Chang *et al.* 1999; Chang & Balice-Gordon, 2000; Meier & Dermietzel, 2006). The present results show the persistence of moderate to dense levels of Cx36-puncta in both dorsal and ventral horn areas of adult spinal cord. This persistence is perhaps not surprising given the numerous brain structures where functional Cx36-containing electrical synapses are present in the adult (Bennett & Zukin, 2004; Connors & Long, 2004; Hormuzdi *et al.* 2004; Meier & Dermietzel, 2006). Particularly striking in adult cord was the widely distributed immunolabelling for Cx36 in laminae IV–VI, the labelling associated with a small subset of neurones scattered in laminae IV–VII and dense collections of Cx36-puncta among neurones in lamina IX. Our anatomical observations suggest that Cx36-containing gap junctions continue to be of importance in adult pools of spinal neurones and possibly in processes in

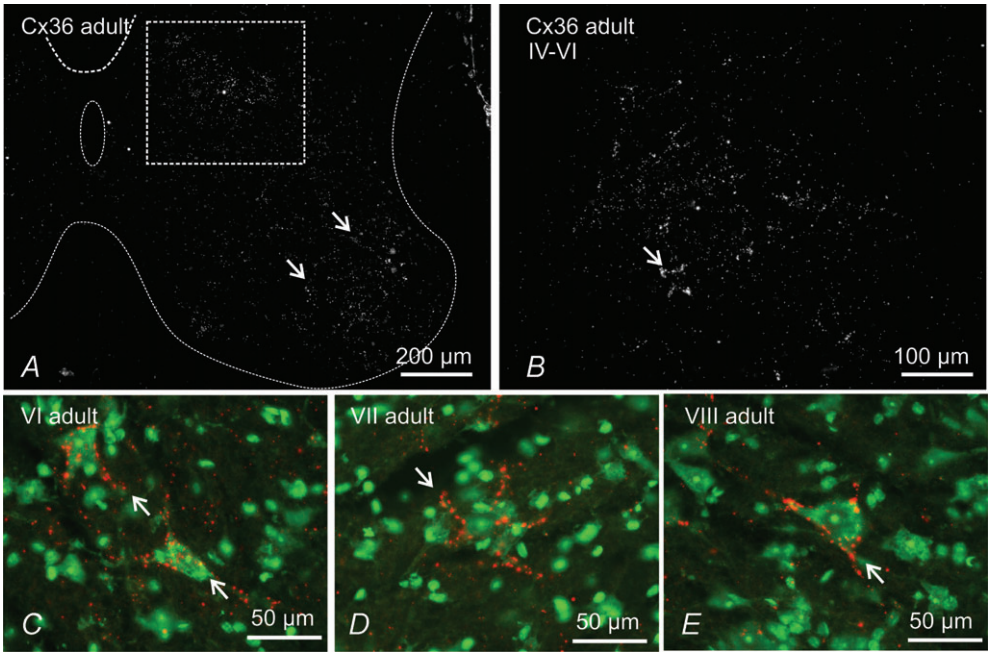

Figure 8. Immunofluorescence labelling of Cx36 in lumbar spinal cord of adult mouse
A, low magnification of deep dorsal horn and the whole of the ventral horn grey matter (outlined by dotted line). Cx36-puncta are distributed throughout, but are most dense in lamina IX (arrows) and within the boxed area straddling the deep dorsal horn and intermediate zone. *B*, magnification of a region corresponding to that of the box in *A*, showing dispersed and clustered Cx36-puncta (arrow). *C–E*, fluorescence Nissl counterstained (green) sections showing examples of Cx36-puncta (red) densely distributed around relatively small neurones (arrows) located in lamina VI (*C*), lamina VII (*D*) and in a mid-region of lamina VIII (*E*).

addition to presynaptic inhibition. In this regard it is noteworthy that there is extensive electrical coupling between motoneurones in very young animals that is largely lost during the second week after birth (Walton & Navarrete, 1991). The re-distribution of Cx36-puncta on motoneurones during development (Fig. 7) presumably reflects changing physiological roles of electrical synapses associated with these cells in the adult, which may be somehow related to the loss of coupling between these neurones during development. The demonstration of Cx36-puncta on motoneurones at P5, an age when these cells are known to be electrically coupled, serves as a positive control for our use of labelling for Cx36 as an indicator of electrical synapse detection. With these considerations, it may be inferred that Cx36-puncta, where present in the adult, reflect functional electrical coupling between spinal neurones such as has been observed between some motoneurones in the adult (Gogan *et al.* 1977).

Because of the present interest in the process of presynaptic inhibition of large diameter primary afferents, dye-coupling between spinal interneurones was investigated only in regions known to contain neurones involved in this process, namely laminae V–VI. These regions contain the GABAergic interneurones that project to the ventral horn and form P boutons on muscle spindle afferents (Hughes *et al.* 2005; discussed below). As shown in Fig. 9, at P11 there is extensive dye-coupling between neurones in these laminae and extensive punctate labelling for Cx36 on dye-coupled neurones. The presence of functional Cx36-containing gap junctions between neurones in these areas is consistent with a role of electrical synapses in presynaptic inhibition. A full appreciation of the identity of dye-coupled neurones in relation to the localization and function of Cx36 in particular neuronal populations will require a more comprehensive analysis.

Role of gap junctions in presynaptic inhibition

Figure 10 shows how Cx36-containing gap junctions might be involved in presynaptic inhibition of group Ia muscle spindle afferents making monosynaptic contacts on motoneurones. For the purposes of the present discussion, the possibility of Cx36-mediated coupling among other spinal cord cell types and afferents is not considered (e.g. Chapman *et al.* 2009). Presynaptic inhibition is believed to involve a three-synapse, two-neurone pathway (Jankowska *et al.* 1981; but see Shreckengost *et al.* 2010) in which glutamatergic sensory afferents activate excitatory first order interneurones. The first order interneurones are thought to be glutamatergic because there is evidence that activation of excitatory glutamatergic interneurones occurs immediately before the onset of presynaptic inhibition (Rudomin, 2009). These neurones then activate a population of GABAergic interneurones that have axo-axonic contacts on primary afferents (see Rudomin, 2009). There is strong electrophysiological and anatomical evidence that deep dorsal horn laminae are the principal locations of GABAergic interneurones mediating presynaptic inhibition of large diameter afferents in the cat and rodent spinal cord (Jankowska *et al.* 1981; Rudomin *et al.* 1987; Maxwell *et al.* 1990; Hughes *et al.* 2005; Betley *et al.* 2009). These interneurones may in part correspond to neurons in the medial laminae IV–VI where we found cells having the capacity for intercellular exchange of neurobiotin, and where neurobiotin-coupled cells were richly endowed with Cx36-puncta (Fig. 9). Based on the foregoing, the

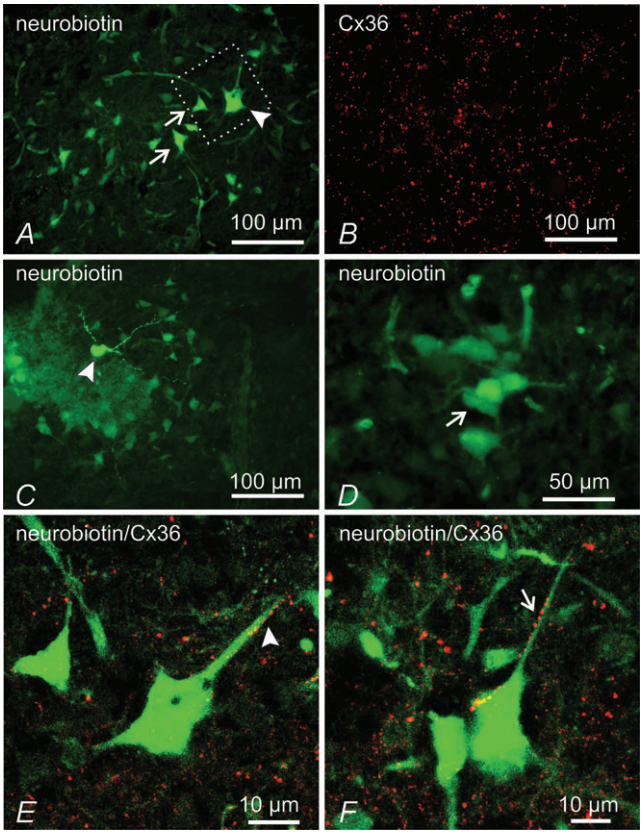

Figure 9. Immunofluorescence labelling of Cx36 (red) associated with neurobiotin-coupled neurones (green) in deep dorsal horn and intermediate zone of mice at P11
A and *B*, low magnification showing a neurobiotin-injected neuron (*A*, arrowhead), giving rise to surrounding neurobiotin-positive neurons (*A*, arrows), and the same field (*B*) showing dense immunolabelling for Cx36 in lamina VI. *C* and *D*, neurobiotin-injected neuron in lamina V (*C*, arrowhead), and higher magnification from an adjacent section showing clusters of neurobiotin-positive neurones (*D*, arrow). *E* and *F*, confocal laser scanning images showing overlays of neurobiotin-positive neurones and immunofluorescence labelling for Cx36, with green/red overlap seen as yellow. The image in *E* is a magnification of the boxed area shown in *A*. Cx36-puncta are seen associated with dendrites and soma of a neurobiotin-injected neurone (*E*, arrowhead) and neurobiotin-coupled neurone (*F*, arrows).

hypothesis presented in Fig. 10 is that GABAergic neurones in deep dorsal horn laminae are gap junctionally coupled and make axo-axonic contacts with large diameter primary afferents and, in particular, Ia spindle afferents. Also depicted in Fig. 10 is the possibility that gap junctions exist between excitatory first order interneurones that activate second order presynaptic inhibitory pathways, but direct evidence for this is presently lacking. However, bearing on this point is that at least some components of the cord dorsum potential are related to activation of excitatory (presumably glutamatergic) interneurones in the dorsal horn (Rudomin, 2009). The depressed CDP observed in the Cx36 knockouts supports equally the possibility that, in the knockout mouse, glutamatergic interneurones lack synchronous robust activity conferred by gap junction coupling.

One of the most emphasised features of inter-neuronal gap junctions is their ability to function as low-pass filters, where longer duration, subthreshold depolarizations, in contrast to spikes, are efficiently transmitted within a network of coupled neurons, allowing synchronization of spike activity of near-threshold neurones (Bennett & Zukin 2004). Equally important, the behaviour of a coupled network will be dependent upon both the nature and duration of the afferent input as well as the intrinsic membrane properties of the coupled neurones (Mann-Metzer & Yarom 1999; Dugué *et al.* 2009; Curti *et al.* 2012). Gap junctions could serve to trigger intrinsic oscillatory currents in coupled neurones, to temporally synchronize action potentials with the onset of afferent input, to prolong activity in the population as the afferent input decays, or to help select a subpopulation of coupled interneurones within a larger population of spinal neurones with similar afferent input. A facilitation of activity within the gap junction coupled networks in Fig. 10 would presumably result in a concerted expression of presynaptic inhibition of primary afferents. This idea is in accord with the suggestion (see Rudomin, 2009) that synchronous activity of subpopulations of interneurones involved in presynaptic inhibition can distribute primary afferent depolarization to selected collaterals of afferents in different spinal locations. It is also in accord with the suggestion that when afferents contact multiple spinal pathways, activity in those displaying synchronous interneuronal activity, e.g. those in presynaptic inhibitory networks, would be promoted over reflex effects mediated through other, unsynchronized, networks (Chavez *et al.* 2012). Accordingly, gap junction coupling may be extensive within subsets of interneurones organized into functionally discrete groups. Based on these considerations, it might be predicted that pharmacological uncoupling of gap junctions in wild-type mice or the loss of Cx36 in transgenic mice would compromise a concerted action of these interneurones on transmission at primary afferents. This proposed mechanism for an essential role of electrical connections between neurones in sensory-evoked presynaptic inhibition is supported by the loss of long-latency inhibition of the MSR in spinal cord preparations from Cx36 knockouts and following bath application of gap junction blockers in cords from wild-type mice. These observations provide strong evidence for the involvement of Cx36-containing gap junctions in the presynaptic control of the synapse between Ia muscle spindle afferents and lumbar motoneurones. The abundance of Cx36-puncta in spinal laminae IV–VI also suggests a role of electrical synapses in the presynaptic control of other segmental reflexes, for example those from tendon organs and spindle secondary afferents. It is noteworthy that gap junctions may also be involved in the presynaptic control of sensory input to dorsal spinocerebellar tract neurones which shares several features of the presynaptic inhibition of Ia terminals on motoneurones. This includes axo-axonic synapses (Walmsley, 1991), sensory-evoked PAD of group I afferent input (Jankowska & Padel, 1984) and GABAergic control of afferent input to dorsal spinocerebellar tract neurones (Hantman & Jessell, 2010).

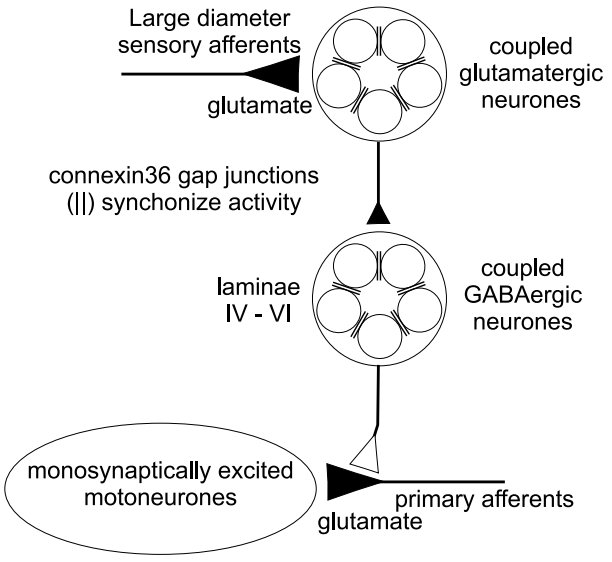

Figure 10. Proposed role of neuronal gap junctions in facilitating presynaptic inhibition
Large diameter sensory afferents contact populations of lumbar spinal interneurones that are excitatory to other interneurones located in intermediate spinal laminae. These second order interneurones release GABA onto the presynaptic terminals of primary afferents causing PAD and a subsequent reduction in glutamate release from sensory afferents. In the circuit depicted here, this presynaptic inhibition results in smaller monosynaptic EPSPs generated in motoneurones by Ia muscle spindle afferents. Gap junctions formed by Cx36 (||) are hypothesized to couple and synchronize activity in interneurone populations responsible for presynaptic inhibition. Ablation of Cx36 or pharmacological inhibition of gap junctions in wild-types results in a severe impairment of the presynaptic regulation of transmission from large diameter sensory afferents.

Interestingly, some previously described laminae V–VI interneurones (Hughes *et al.* 2005) are GAD65 positive and make P-bouton (axo-axonic) contacts with primary afferent terminals in the ventral horn. Since Ia muscle spindle afferents are the only sensory afferents with extensive monosynaptic connections on motoneurones, the present results on MSR inhibition raise the likelihood that at least some of the interneurones described by Hughes *et al.* (2005) are coupled by electrical synapses. Recent reports, however, suggest that at least in very young animals these spinal regions also contain populations of GABAergic interneurones not involved in presynaptic inhibition (Wilson *et al.* 2010). There is also strong physiological evidence that some GABAergic interneurones may be involved in both presynaptic inhibition of afferent transmission and postsynaptic inhibition of motoneurones (Rudomin *et al.* 1990; see Rudomin, 2009). Full identification of GABAergic interneurone populations in these laminae and the organization of gap junctionally coupled networks among them remain to be determined.

Presynaptic inhibition of large diameter muscle and cutaneous afferents in the spinal cord is a regulatory process in which sensory afferent activity results in reduced transmitter release from the same and other afferents and is an integral component of reflex control during locomotion and other movements (Rossignol *et al.* 2006; Rudomin 2009). Studies during locomotion, however, indicate the existence of an additional source of presynaptic inhibition that arises from the operation of central pattern generating circuitry and can occur without sensory stimulation (discussed in Gosgnach *et al.* 2000). It remains an attractive possibility that electrical synapses play a similar role in this centrally evoked presynaptic inhibition as the one described here in sensory-evoked presynaptic inhibition. Dysregulation of presynaptic inhibition is believed to be one of the major factors in human spasticity arising from spinal cord injury, and drugs that augment presynaptic inhibition, such as baclofen, are a mainstay in treatment of spasticity (Simon & Yelnick, 2010). Recently, it has been suggested that injury-induced changes in connexin36 expression in spinal cord contribute to spasticity (Yates *et al.* 2011). The present results directly linking Cx36 to presynaptic inhibition, a process known to malfunction in human spasticity, raise the possibility that this condition arises in part from dysfunction of gap junctionally coupled networks involved in presynaptic inhibition.

References

Allison DW, Wilcox RS, Ellefsen KL, Askew CE, Hansen DM, Wilcox JD, Sandoval SS, Eggett DL, Yanagawa Y & Steffensen SC (2011). Mefloquine effects on ventral tegmental area dopamine and GABA neuron inhibition: a physiologic role for connexin-36 gap junctions. *Synapse* **65**, 805–813.

Bagust J, Green KA & Kerkut GA (1981). Strychnine sensitive inhibition in the dorsal horn of mammalian spinal cord. *Brain Res* **217**, 425–429.

Bagust J, Forsythe D & Kerkut GA (1985). Demonstration of the synaptic origin of primary afferent depolarisation (PAD) in the isolated spinal cord of the hamster. *Brain Res* **341**, 385–389.

Bennett MVL (1997). Gap junctions as electrical synapses. *J Neurocytol* **26**, 349–366.

Bennett MV & Zukin RS (2004). Electrical coupling and neuronal synchronization in the mammalian brain. *Neuron* **41**, 495–511.

Betley JN, Wright CV, Kawaguchi Y, Erdelyi F, Szabo G, Jessell TM & Kaltschmidt JA (2009). Stringent specificity in the construction of a GABAergic presynaptic inhibitory circuit. *Cell* **139**, 161–174.

Carlin KP, Jiang Z & Brownstone RM (2000). Characterization of calcium currents in functionally mature mouse spinal motoneurons. *Eur J Neurosci* **12**, 1624–1634.

Chapman RJ, Cilia La Corte PF, Asghar AUR & King A (2009). Network-based activity induced by 4-aminopyridine in rat dorsal horn in vitro is mediated by both chemical and electrical synapses. *J Physiol* **587**, 2499–2510.

Chang Q & Balice-Gordon RJ (2000). Gap junctional communication among developing and injured motor neurons. *Brain Res Brain Res Rev* **32**, 242–249.

Chang Q, Gonzalez M, Pinter MJ & Balice-Gordon RJ (1999). Gap junctional coupling and patterns of connexin expression among neonatal rat lumbar spinal motor neurons. *J Neurosci* **19**, 10813–10828.

Chávez D, Rodríguez E, Jiménez I & Rudomin P (2012). Changes in correlation between spontaneous activity of dorsal horn neurones lead to differential recruitment of inhibitory pathways in the cat. *J Physiol* **590**, 1563–1584.

Clarke WT, Edwards B, McCullagh KJ, Kemp MW, Moorwood C, Sherman DL, Burgess M & Davies KE(2010). Syncoilin modulates peripherin filament networks and is necessary for large-calibre motor neurons. *J Cell Sci* **123**, 2543–2552.

Coleman AM & Sengelaub DR (2002). Patterns of dye coupling in lumbar motor nuclei of the rat. *J Comp Neurol* **454**, 34–41.

Connors BW & Long MA (2004). Electrical synapses in the mammalian brain. *Annu Rev Neurosci* **27**, 393–418.

Cruikshank SJ, Hopperstad M, Younger M, Connors BW, Spray DC & Srinivas M (2004). Potent block of Cx36 and Cx50 gap junction channels by mefloquine. *Proc Natl Acad Sci U S A* **101**, 12364–12369.

Curtis DR, Duggan AW, Felix D & Johnston GA (1971). Bicuculline, an antagonist of GABA and synaptic inhibition in the spinal cord of the cat. *Brain Res* **32**, 69–96.

Curti S, Hoge G, Nagy JI & Pereda AE (2012). Synergy between electrical coupling and membrane properties promotes strong synchronization of neurons of the mesencephalic trigeminal nucleus. *J Neurosci* **32**, 4341–4359.

Dai Y, Carlin KP, Li X, McMahon DG, Brownstone RM & Jordan LM (2009). Electrophysiological and pharmacological properties of locomotor activity-related neurons in cfos-EGFP mice. *J Neurophysiol* **102**, 3365–3383.

Deans MR, Gibson JR, Sellitto C, Connors BW & Paul DL (2001). Synchronous activity of inhibitory networks in neocortex requires electrical synapses containing connexin36. *Neuron* **16**, 477–485.

Deshpande SB & Warnick JE (1988). Temperature-dependence of reflex transmission in the neonatal rat spinal cord, in vitro: influence on strychnine- and bicuculline-sensitive inhibition. *Neuropharmacology* **27**, 1033–1037.

Drummond GB (2009). Reporting ethical matters in *The Journal of Physiology*: standards and advice. *J Physiol* **587**, 713–719.

Duflocq A, Le Bras B, Bullier E, Couraud F & Davenne M (2008). Nav1.1 is predominantly expressed in nodes of Ranvier and axon initial segments. *Mol Cell Neurosci* **39**, 180–192.

Dugué GP, Brunel N, Hakim V, Schwartz E, Chat M, Lévesque M, Courtemanche R, Léna C & Dieudonné S (2009). Electrical coupling mediates tunable low-frequency oscillations and resonance in the cerebellar Golgi cell network. *Neuron* **61**, 126–139.

Eccles JC, Schmidt R & Willis WD (1963). Pharmacological studies on presynaptic inhibition. *J Physiol* **168**, 500–530.

Enríquez M, Jiménez I & Rudomin P (1996). Segmental and supraspinal control of synaptic effectiveness of functionally identified muscle afferents in the cat. *Exp. Brain Res* **107**, 391–404.

Frisch C, De Souza-Silva MA, Söhl G, Güldenagel M, Willecke K, Huston JP & Dere E (2005). Stimulus complexity dependent memory impairment and changes in motor performance after deletion of the neuronal gap junction protein connexin36 in mice. *Behav Brain Res* **157**, 177–185.

Gogan P, Gueritaud JP, Horcholle-Bossavit G & Tyc-Dumont S (1977). Direct excitatory interactions between spinal motoneurones of the cat. *J Physiol* **272**, 755–767.

Gosgnach S, Quevedo J, Fedirchuk B & McCrea DA (2000). Depression of group Ia monosynaptic EPSPs in cat hindlimb motoneurones during fictive locomotion. *J Physiol* **526**, 639–652.

Hantman AW & Jessell TM (2010). Clarke's column neurons as the focus of a corticospinal corollary circuit. *Nat Neurosci* **13**, 1233–1237.

Hinckley CA & Ziskind-Conhaim L (2006). Electrical coupling between locomotor-related excitatory interneurons in the mammalian spinal cord. *J Neurosci* **26**, 8477–8483.

Hormuzdi SG, Filippov MA, Mitropoulou G, Monyer H & Bruzzone R (2004). Electrical synapses: a dynamic signaling system that shapes the activity of neuronal networks. *Biochim Biophys Acta* **1662**, 113–137.

Hughes DI, Mackie M, Nagy GG, Riddell JS, Maxwell DJ, Szabo G, Erdelyi F, Veress G, Szucs P, Antal M & Todd AJ (2005). P boutons in lamina IX of the rodent spinal cord express high levels of glutamic acid decarboxylase-65 and originate from cells in deep medial dorsal horn. *Proc Natl Acad Sci U S A* **102**, 9038–9043.

Jankowska E, McCrea D, Rudomin P & Sykova E (1981). Observations on neuronal pathways subserving primary afferent depolarization. *J Neurophysiol* **46**, 506–516.

Jankowska E & Padel Y (1984). On the origin of presynaptic depolarization of group I muscle afferents in Clarke's column in the cat. *Brain Res* **295**, 195–201.

Jiang Z, Carlin KP & Brownstone RM (1999). An in vitro functionally mature mouse spinal cord preparation for the study of spinal motor networks. *Brain Res* **816**, 493–499.

Juszczak GR & Swiergiel AH (2009). Properties of gap junction blockers and their behavioural, cognitive and electrophysiological effects: animal and human studies. *Prog Neuropsychopharmacol Biol Psychiatry* **33**, 181–198.

Kamasawa N, Furman CS, Davidson KG, Sampson JA, Magnie AR, Gebhardt BR, Kamasawa M, Yasumura T, Zumbrunnen JR, Pickard GE, Nagy JI & Rash JE (2006). Abundance and ultrastructural diversity of neuronal gap junctions in the OFF and ON sublaminae of the inner plexiform layer of rat and mouse retina. *Neuroscience* **142**, 1093–1117.

Kandler K & Katz LC (1995). Neuronal coupling and uncoupling in the developing nervous system. *Curr Opin Neurobiol* **1**, 98–105.

Kiehn O & Tresch MC (2002). Gap junctions and motor behavior. *Trends Neurosci* **25**, 108–115.

Kremer E & Lev-Tov A (1998). GABA-receptor – independent dorsal root afferents depolarization in the neonatal rat spinal cord. *J Neurophysiol* **79**, 2581–2592.

Li X, Olson C, Lu S, Kamasawa N, Yasumura T, Rash JE & Nagy JI (2004). Neuronal connexin36 association with zonula occludens-1 protein (ZO-1) in mouse brain and interaction with the first PDZ domain of ZO-1. *Eur J Neurosci* **19**, 2132–2146.

Lemieux M, Cabana T & Pflieger JF (2010). Distribution of the neuronal gap junction protein Connexin36 in the spinal cord enlargements of developing and adult opossums, *Monodelphis domestica*. *Brain Behav Evol* **75**, 23–32.

Lidierth M & Wall PD (1996). Synchronous inherent oscillations of potentials within the rat lumbar spinal cord. *Neurosci Lett* **220**, 25–28.

Logan SD, Pickering AE, Gibson IC, Nolan MF & Spanswick D (1996). Electrotonic coupling between rat sympathetic preganglionic neurones *in vitro*. *J Physiol* **495**, 491–502.

Mann-Metzer P & Yarom Y (1999). Electrotonic coupling interacts with intrinsic properties to generate synchronized activity in cerebellar networks of inhibitory interneurons. *J Neurosci* **19**, 3298–3306.

Manjarrez E, Jimenez I & Rudomin P (2003). Intersegmental synchronization of spontaneous activity of dorsal horn neurons in the cat spinal cord. *Exp Brain Res* **148**, 401–413.

Marina N, Becker DL & Gilbey MP (2008). Immunohistochemical detection of connexin36 in sympathetic preganglionic and somatic motoneurons in the adult rat. *Auton Neurosci* **139**, 15–23.

Maxwell DJ, Christie WM, Short AD & Brown AG (1990). Direct observations of synapses between GABA-immunoreactive boutons and muscle afferent terminals in lamina VI of the cat's spinal cord. *Brain Res* **530**, 215–222.

McCrea DA, Shefchyk SJ & Carlen PC (1990). Large reductions in composite EPSP amplitude following conditioning stimulation are not accounted for by increased conductances in motoneurons. *Neurosci Let* **109**, 117–122.

McCrea D, Bautista Guzman W, Nagy J & Fedirchuk B (2009). Presynaptic inhibition in neonatal spinal cord is impaired in connexin36 knockout mice. *2009 Abstract Viewer/Itinerary Planner*, Programme No. 421.14. Society for Neuroscience, Washington, DC.

Mendell L (1972). Properties and distribution of peripherally evoked presynaptic hyperpolarization in cat lumbar spinal cord. *J Physiol* **226**, 769–792.

Meier C & Dermietzel R (2006). Electrical synapses–gap junctions in the brain. *Results Probl Cell Differ* **43**, 99–128.

Nagy J & Dermietzel R (2000). Gap junctions and connexins in the mammalian central nervous system. In *Advances in Molecular and Cell Biol*, vol. 30, ed. Hertzberg, EI, pp 323–396. JAI Press, Greenwich, CT.

Nagy JI, Dudek FE & Rash JE (2004). Update on connexins and gap junctions in neurons and glia in the mammalian nervous system. *Brain Res Brain Res Rev* **47**, 191–215.

Placantonakis DG, Bukovsky AA, Zeng XH, Kiem HP & Welsh JP (2004). Fundamental role of inferior olive connexin 36 in muscle coherence during tremor. *Proc Nat Acad Sci U S A* **101**, 7164–7169.

Rash JE, Dillman RK, Bilhartz BL, Duffy HS, Whalen LR & Yasumura T (1996). Mixed synapses discovered and mapped throughout mammalian spinal cord. *Proc Natl Acad Sci U S A* **93**, 4235–4239.

Rash JE, Olson CO, Davidson KG, Yasumura T, Kamasawa N & Nagy JI (2007*a*). Identification of connexin36 in gap junctions between neurons in rodent locus coeruleus. *Neuroscience* **147**, 938–956.

Rash JE, Olson CO, Pouliot WA, Davidson KG, Yasumura T, Furman CS, Royer S, Kamasawa N, Nagy JI & Dudek FE (2007*b*). Connexin36 vs. connexin32, "miniature" neuronal gap junctions, and limited electrotonic coupling in rodent suprachiasmatic nucleus. *Neuroscience* **149**, 350–371.

Rash JE, Pereda A, Kamasawa N, Furman CS, Yasumura T, Davidson KG, Dudek FE, Olson C, Li X & Nagy JI (2004). High-resolution proteomic mapping in the vertebrate central nervous system, close proximity of connexin35 to NMDA glutamate receptor clusters and co-localization of connexin36 with immunoreactivity for zonula occludens protein-1 (ZO-1). *J Neurocytol* **33**, 131–51.

Rash JE, Yasumura T, Davidson KG, Furman CS, Dudek FE & Nagy JI (2001*a*). Identification of cells expressing Cx43, Cx30, Cx26, Cx32 and Cx36 in gap junctions of rat brain and spinal cord. *Cell Commun Adhes* **8**, 315–320.

Rash JE, Yasumura T, Dudek FE & Nagy JI (2001*b*). Cell-specific expression of connexins and evidence of restricted gap junctional coupling between glial cells and between neurons. *J Neurosci* **21**, 1983–2000.

Rossignol S, Dubuc R & Gossard JP (2006). Dynamic sensorimotor interactions in locomotion. *Physiol Rev* **86**, 89–154.

Rudomin P (2009). In search of lost presynaptic inhibition. *Exp Brain Res* **196**, 139–151.

Rudomin P, Jimenez I, Quevedo J & Solodkin M (1990). Pharmacologic analysis of inhibition produced by last-order intermediate nucleus interneurons mediating nonreciprocal inhibition of motoneurons in cat spinal cord. *J Neurophysiol* **63**, 147–160.

Rudomin P & Schmidt RF (1999). Presynaptic inhibition in the vertebrate spinal cord revisited. *Exp Brain Res* 129, 1–37.

Rudomin P, Solodkin M & Jimenez I (1987). Synaptic potentials of primary afferent fibers and motoneurons evoked by single intermediate nucleus interneurons in the cat spinal cord. *J Neurophysiol* **57**, 1288–1313.

Shreckengost J, Calvo J, Quevedo J & Hochman S (2010). Bicuculline-sensitive primary afferent depolarization remains after greatly restricting synaptic transmission in the mammalian spinal cord. *J Neurosci* **30**, 5283–5288.

Simon O & Yelnik AP (2010). Managing spasticity with drugs. *Eur J Phys Rehabil Med* **46**, 401–410.

Thompson SW & Wall PD (1996). The effect of GABA and 5-HT receptor antagonists on rat dorsal root potentials. *Neurosci Lett* **217**, 153–156.

Van Der Giessen RS, Koekkoek SK, van Dorp S, De Gruijl JR, Cupido A, Khosrovani S, Dortland B, Wellershaus K, Degen J, Deuchars J, Fuchs EC, Monyer H, Willecke K, De Jeu MT, De Zeeuw CI (2008). Role of olivary electrical coupling in cerebellar motor learning. *Neuron* **58**, 599–612.

Walmsley B (1991). Central synaptic transmission: studies at the connection between primary afferent fibres and dorsal spinocerebellar tract (DSCT) neurones in Clarke's column of the spinal cord. *Prog Neurobiol* **36**, 391–423.

Walton KD & Navarrete R (1991). Postnatal changes in motoneurone electrotonic coupling studied in the *in vitro* rat lumbar spinal cord. *J Physiol* **433**, 283–305.

Wang Z, Li L, Goulding M & Frank E (2008). Early postnatal development of reciprocal Ia inhibition in the murine spinal cord. *J Neurophysiol* **100**, 185–196.

Willis WD (2006). John Eccles' studies of spinal cord presynaptic inhibition. *Prog Neurobiol* **78**, 189–214.

Wilson JM, Blagovechtchenski E & Brownstone RM (2010). Genetically defined inhibitory neurons in the mouse spinal cord dorsal horn: a possible source of rhythmic inhibition of motoneurons during fictive locomotion. *J Neurosci* **30**, 1137–1148.

Wilson JM, Cowan AI & Brownstone RM (2007). Heterogeneous electrotonic coupling and synchronization of rhythmic bursting activity in mouse Hb9 Interneurons. *J Neurophysiol* **98**, 2370–2381.

Wong SM, Cheng G, Homanics GE & Kendig JJ (2001). Enflurane actions on spinal cords from mice that lack the beta3 subunit of the $GABA_A$ receptor. *Anesthesiology* **95**, 154–164.

Yates C, Garrison K, Reese NB, Charlesworth A & Garcia-Rill E (2011). Novel mechanism for hyperreflexia and spasticity. *Prog Brain Res* **188**, 167–180.

Zlomuzica A, Viggiano D, Degen J, Binder S, Ruocco LA, Sadile AG, Willecke K, Huston JP & Dere E (2012). Behavioral alterations and changes in Ca/calmodulin kinase II levels in the striatum of connexin36 deficient mice. *Behav Brain Res* **226**, 293–300.

Author contributions

All experiments were performed in the laboratories of the Spinal Cord Research Centre at the University of Manitoba. Most of the data were collected and analysed by W.B. with the assistance of

the other authors. The dye coupling experiments were performed with Y.D. and W.B. D.M., J.N. and W.B. contributed equally to the writing and revision of the manuscript. All authors approved the final version of the manuscript.

Acknowledgements

This work was supported by Canadian Institutes of Health Research grants to D.M. (MOP 37756) and J.I.N. (MOP 106598) and by National Institutes of Health (NS31027, NS44010, NS44295) to J. E. Rash with sub-award to J.I.N. We thank David Paul (Harvard) for providing Cx36 knockout mouse breeding pairs, Dr Fedirchuk for providing electrophysiology facilities, Dr Eugene Zaporozhets for helpful guidance on the dissection techniques, Dr B. D. Lynn for genotyping transgenic mice, and B. McLean and S. McCartney for excellent technical assistance. W.B. was supported by a Manitoba Health Research Council Studentship.